THE JOURNAL OF BIOLOGICAL CHEMISTRY VOL. 288, NO. 40, pp. 28524–28534, October 4, 2013

Angiopoietin-like Protein 4 Inhibition of Lipoprotein Lipase

*EVIDENCE FOR REVERSIBLE COMPLEX FORMATION**

Received for publication, June 27, 2013, and in revised form, August 6, 2013 Published, JBC Papers in Press, August 19, 2013, DOI 10.1074/jbc.M113.497602

Michael J. Lafferty[‡], Kira C. Bradford[§], Dorothy A. Erie[§], and Saskia B. Neher[‡1]

From the Departments of [‡]Biochemistry and Biophysics, and [§]Chemistry, University of North Carolina, Chapel Hill, North Carolina 27599

Background: Lipoprotein lipase (LPL) clears triglycerides from the blood, and angiopoietin-like protein 4 (ANGPTL4) inhibits LPL activity.
Results: Inhibited LPL is in a complex with ANGPTL4, and upon dissociation LPL regains activity.
Conclusion: ANGPTL4 is a reversible, noncompetitive inhibitor of LPL, not an unfolding molecular chaperone as reported previously.
Significance: Understanding the mechanism of LPL inhibition supports efforts to develop new therapies for hypertriglyceridemia.

Elevated triglycerides are associated with an increased risk of cardiovascular disease, and lipoprotein lipase (LPL) is the rate-limiting enzyme for the hydrolysis of triglycerides from circulating lipoproteins. The N-terminal domain of angiopoietin-like protein 4 (ANGPTL4) inhibits LPL activity. ANGPTL4 was previously described as an unfolding molecular chaperone of LPL that catalytically converts active LPL dimers into inactive monomers. Our studies show that ANGPTL4 is more accurately described as a reversible, noncompetitive inhibitor of LPL. We find that inhibited LPL is in a complex with ANGPTL4, and upon dissociation, LPL regains lipase activity. Furthermore, we have generated a variant of ANGPTL4 that is dependent on divalent cations for its ability to inhibit LPL. We show that LPL inactivation by this regulatable variant of ANGPTL4 is fully reversible after treatment with a chelator.

LPL[2] is the key enzyme involved in regulation of serum lipid levels. LPL is a secreted enzyme that functions on the surface of the capillary endothelium where it hydrolyzes triglycerides contained within circulating chylomicrons and very low density lipoprotein to provide free fatty acids to tissues (1). Familial LPL deficiency is a rare but serious condition that results in extremely high serum triglyceride levels (severe hypertriglyceridemia) that lead to eruptive xanthomas, lipemia retinalis, and pancreatitis, resulting in a poor health-related quality of life and early mortality (2). Mildly elevated serum triglycerides are more common, with over one-third of Americans suffering from some level of hypertriglyceridemia (3). Hypertriglyceridemia is associated with increased risk of cardiovascular disease (4) along with predicting the development of type 2 diabetes mellitus (5). Current research is focused on finding ways to maintain or increase LPL activity to alleviate the effects of hypertriglyceridemia (6, 7).

LPL belongs to a superfamily of lipases that includes the mammalian endothelial, pancreatic, and hepatic lipases (8). There is no crystal structure for LPL, but due to high sequence similarity with pancreatic lipase, its crystal structure can serve as a model to provide information about the structure-function relationships that govern LPL activity (9, 10). The LPL protein is composed of two structurally distinct domains that are connected by a short linker. The N-terminal domain includes the active site, and homology modeling suggests that it takes on an α/β-hydrolase fold (9). The C-terminal domain is modeled as a β-sandwich and is responsible for binding the cell surface protein glycosylphosphatidylinositol-anchored high density lipoprotein-binding protein 1 (GPIHBP1) (9–11). LPL is only active as a homodimer, and the two subunits are oriented in a head to tail fashion such that the N-terminal domain of one LPL monomer faces the C-terminal domain of the other (12, 13).

Because of its key role in regulating lipid homeostasis, LPL activity must be tightly coordinated with nutritional status. LPL regulation is tissue-specific such that upon fasting LPL activity decreases in adipose tissue and increases in muscle tissue (14). Tissue-specific regulation of LPL is thus thought to direct fatty acids to adipose tissue for storage when lipids are plentiful and to muscle tissues for fuel when lipids are scarce. ANGPTL4 is a secreted protein that directly regulates LPL activity (15). Mice lacking ANGPTL4 show increased LPL activity and decreased plasma triglycerides, whereas mice overexpressing ANGPTL4 display elevated plasma triglycerides and reduced LPL activity (16). ANGPTL4 inhibition of LPL activity is nutritionally responsive and tissue-specific, as ANGPTL4 expression is induced in adipose tissue in response to fasting (15, 17).

ANGPTL4 is a two domain protein, and each domain has been shown to have a distinct biological function. The N-terminal domain is a coiled-coil that mediates oligomerization of the protein, and the C-terminal portion is a fibrinogen-like domain (18). After ANGPTL4 is secreted, these domains are

* This work was supported by a grant from the Pew Foundation (to S. B. N.).
[1] To whom correspondence may be addressed: Dept. of Biochemistry and Biophysics, University of North Carolina at Chapel Hill, 120 Mason Farm Rd., CB 7260, Chapel Hill, NC 27599. Tel.: 919-966-9550; E-mail: neher@email.unc.edu.
[2] The abbreviations used are: LPL, lipoprotein lipase; ANGPTL4, angiopoietin-like protein 4; GPIHBP1, glycosylphosphatidylinositol-anchored high density lipoprotein-binding protein 1; AFM, atomic force microscopy; MID1, metal-interface-design 1; BisTris, 2-[bis(2-hydroxyethyl)amino]-2-(hydroxymethyl)propane-1,3-diol.

cleaved apart by the action of pro-protein convertases (18, 19). The N-terminal domain inhibits LPL activity, and cleavage of the two domains enhances this inhibition (18, 20, 21). A mechanism for LPL inhibition was described, in which ANGPTL4 was termed an unfolding molecular chaperone of LPL (22). In that study, it was reported that ANGPTL4 inhibits LPL activity by promoting a conformational change in LPL such that active LPL dimers dissociate and form inactive monomers (22). Active LPL dimers are known to undergo both reversible dissociation that results in rapid exchange of subunits and irreversible dissociation that results in inactive monomers (12, 23). Irreversible dissociation can be induced by heat or denaturant and results in loss of catalytic activity and a change in secondary structure (23). The ANGPTL4-induced conformational change in LPL was reported to be akin to irreversible dissociation (22).

We set out to uncover the mechanism by which this conformational change occurs and found instead that ANGPTL4 inhibits LPL by a reversible, noncompetitive mechanism. Inhibited LPL was found in a complex with ANGPTL4, and superstoichiometric ratios of ANGPTL4/LPL were required for complete inhibition. These findings may have considerable *in vivo* significance in light of recent data showing that, in humans, serum ANGPTL4 levels do not correlate with plasma triglyceride levels and that LPL travels bidirectionally across endothelial cells (24, 25). These data have led to the suggestion that ANGPTL4 could inhibit LPL in the subendothelial space rather than on the endothelial surface (25). Here, we report our data showing a noncompetitive mechanism for ANGPTL4 inhibition of LPL and discuss its possible physiological implications.

EXPERIMENTAL PROCEDURES

Protein Purification, LPL—Bovine LPL was purified from fresh cow's milk as described and stored at −80 °C (26).

ANGPTL4—Amino acids 26–161 of ANGPTL4 (the N-terminal coiled-coil domain) were cloned into pET16b (Novagen) with an N-terminal His tag followed by a GST tag and a tobacco etch virus cleavage site. Protein was expressed in BL21 (DE3) cells, and cells were grown to an A_{600} of 0.5 at 37 °C and then induced with 0.1 mM isopropyl 1-thio-β-D-galactopyranoside for 16 h at 18 °C. Cells were pelleted at 4000 × *g*, suspended in buffer A (20 mM Tris, pH 7.5, 500 mM NaCl, 40 mM imidazole) with 1× Complete EDTA-free protease inhibitors (Roche Applied Science), and lysed in a Nano DeBEE Laboratory homogenizer (BEE International) at 20,000 p.s.i. The lysate was cleared at 34,000 × *g* for 20 min and applied to a nickel-nitrilotriacetic acid resin (Qiagen) that had been pre-equilibrated with buffer A. Resin was washed with 10 column volumes of buffer B (20 mM Tris, pH 7.5, 500 mM NaCl, 80 mM imidazole) and 10 column volumes of buffer C (20 mM Tris, pH 7.5, 150 mM NaCl, 80 mM imidazole). Protein was eluted with buffer C containing an additional 200 mM imidazole. DTT was added to pooled eluate fractions to a final concentration of 5 mM, and tobacco etch virus protease was added to 32 μg/ml to cleave the N-terminal tags. Protein fractions were dialyzed into Mono S start buffer (20 mM Tris, pH 7.5, 100 mM NaCl), injected onto a 1-ml Mono S 5/50 GL column (GE Healthcare) pre-equilibrated with start buffer, and eluted over 20 column volumes using a linear gradient to start buffer containing 2 M NaCl. Fractions containing ANGPTL4 were pooled and buffer-exchanged into HisTrap start buffer (20 mM Tris, pH 7.5, 300 mM NaCl, 40 mM imidazole), injected into a 1-ml HisTrap HP column (GE Healthcare), and eluted with an imidazole gradient (40–500 mM) in HisTrap buffer over 30 column volumes. Fractions containing clean ANGPTL4 were pooled and buffer-exchanged into storage buffer (20 mM Tris, pH 7.5, 300 mM NaCl) and stored at −80 °C. Purified ANGPTL4 was a mixture of monomers and disulfide-bonded dimers and tetramers.

MID1-ANGPTL4—The two cysteine residues of ANGPTL4 (Cys-76 and Cys-80) were mutated to serine residues using site-directed mutagenesis. Previous studies have shown that ANGPTL4 (C76S/C80S) inhibits LPL with the same potency as WT-ANGPTL4 (27), which we confirmed independently (data not shown). Oligonucleotides designed to encode amino acids comprising the MID1 tag (28) (SPLAQQIKNIHSFIHQAKAAGRMDEVRTLQENLHQLMHEYFQ) were added to the 5′ end of the coding sequence for ANGPTL4(26–161) by overlap extension PCR, creating an N-terminal MID1-tagged ANGPTL4 construct. The MID1-ANGPTL4 construct was cloned into pET41a (Novagen) at the NdeI and XhoI sites. Protein was expressed and purified as stated above using a nickel-nitrilotriacetic acid column but eluted in buffer B containing an additional 300 mM imidazole. Fractions containing clean MID1-ANGPTL4 were pooled, and EDTA was added to a final concentration of 0.5 mM and incubated at 4 °C for 16 h. Protein was concentrated using a Centricon concentrator (Amicon) and further purified using a HiLoad 16/200 Superdex 200 column (GE Healthcare) pre-equilibrated with storage buffer (20 mM Tris, pH 7.5, 300 mM NaCl). Purified MID1-ANGPTL4 was stored at −80 °C.

Heparin Chromatography—0.5 nmol (100 nM) of bovine LPL was incubated on ice, at 37 °C, or with 2.4 μM ANGPTL4 for 20 min in heparin buffer (10 mM BisTris, pH 6.5, 10% glycerol, 0.5 M NaCl). A control reaction, containing only ANGPTL4, was also incubated on ice for 20 min. After 20 min, column loads were assayed for LPL activity and then immediately injected onto a 1-ml HiTrap heparin HP column (GE Healthcare) that was pre-equilibrated with heparin buffer. After a 10-ml wash with heparin buffer, 1-ml fractions were eluted from the column by a linear salt gradient over 30 ml from 0.5 to 2 M NaCl in heparin buffer. Fractions were assayed for lipase activity and analyzed by Western blot.

LPL Activity Assay—Lipase activity was measured using a SpectraMax M5 microplate reader (Molecular Devices) and black-walled, clear-bottom, 96-well plates (Corning Glass). Assays were conducted in a total of 100 μl containing 5 nM LPL in assay buffer (20 mM Tris, pH 8.0, 150 mM NaCl, 0.2% fatty-acid free BSA, 0.01% Anzergent 3-16) and 10 μM of the fluorescent substrate 1,2-di-*O*-lauryl-*rac*-glycero-3-(glutaric acid 6-methylresofurin ester) (Sigma). Substrate hydrolysis was measured as the initial increase in fluorescence over 60 s using an excitation wavelength of 529 nm, and reading emission at 600 nm with a 590-nm cutoff filter. Assays were conducted at 25 °C and measured in triplicate. In each assay, initial LPL activity was blanked by subtracting a buffer control (containing 1,2-di-*O*-lauryl-*rac*-glycero-3-(glutaric acid 6-methylresofurin ester) without LPL) and was normalized by dividing the

initial rate of inhibited LPL activity by the initial rate of uninhibited LPL activity. In this way we corrected for the spontaneous loss of LPL lipase activity. Activity assays for the measurement of K_i were assayed as above but with 1 mM deoxycholate added to the assay buffer and between 0.16 and 20 μM substrate.

LPL Inhibition Reactions—The LPL inhibition with the ANGPTL4 time course experiment was conducted with 100 nM LPL and between 0 and 1.6 μM ANGPTL4 in buffer containing 20 mM Tris, pH 7.5, 300 mM NaCl, 1 mM deoxycholate. Reactions were incubated on ice for up to 6 h. Aliquots of the inhibition reactions were assayed for lipase activity as above. LPL inhibition with MID1-ANGPTL4 was conducted with 100 nM LPL and 3.2 μM MID1-ANGPTL4 in 20 mM Tris, pH 7.5, 300 mM NaCl, 5 mM deoxycholate, and 30 μM nickel sulfate at 37 °C. After 45 min, aliquots were tested for lipase activity, and then EDTA was added to a final concentration of 1 mM to chelate the nickel ions. After 15 min with EDTA, aliquots were again tested for lipase activity. Inhibition reactions used for the determination of K_i were conducted at room temperature with 12 nM LPL and between 0 and 38.9 μM ANGPTL4 in 20 mM Tris, pH 7.5, 300 mM NaCl, and 1 mM deoxycholate. Inhibition reactions were incubated for 10 min and then diluted into assay buffer as described above to a final concentration of 5 nM LPL and between 0 and 16.2 μM ANGPTL4.

Thermal Inactivation and Thermofluor Assay—100 nM LPL was incubated in 10 mM BisTris, pH 6.5, 500 mM NaCl, 10% glycerol with or without 1 mM deoxycholate at 4, 25, or 37 °C. At 0, 15, 30, and 60 min, aliquots of the LPL reaction were diluted 20× into assay buffer, and initial rates of fluorescent substrate hydrolysis were measured as above. For the thermofluor assay (29), 20 μl of 900 nM LPL was incubated in 10 mM BisTris, pH 6.5, 500 mM NaCl, and 10% glycerol with 6× SYPRO Orange (Sigma). Assays were conducted in quadruplicate in a 384-well real time PCR plate covered with optically clear sealing film. The plate was incubated at 37 °C in a 7900HT Fast Real Time PCR machine (Applied Biosystems) for 2 h taking fluorescent measurements every 7 s.

Western Blots—Heparin chromatography eluate fractions or LPL/ANGPTL4 cross-linking reactions were separated using SDS-PAGE (12%), transferred to PVDF, blocked with 5% milk in TBS-T, incubated with anti-ANGPTL4 (BioVendor RD181073100-01) at 1:5000 in 2.5% milk/TBS-T or anti-LPL (Santa Cruz Biotechnology sc-32885) at 1:1000 in 2.5% milk/TBST. Blots were washed, incubated with anti-rabbit HRP secondary antibody at 1:20,000 in 2.5% milk/TBST, washed, and exposed to ECL substrate (ADVANSTA Western Bright, BioExpress), and proteins were detected with autoradiography film.

Calculation of K_i—The rate of substrate hydrolysis, recorded as relative fluorescence units/s, was plotted as a function of substrate concentration. Data were fitted to the rate equation for noncompetitive inhibition: $v = V_{max}\cdot[S]/\{(K_m\cdot(1 + [I]/K_i)) + ([S]\cdot(1 + [I]/K_i))\}$, where V_{max} is the un-inhibited maximum rate of substrate hydrolysis; K_m is the Michaelis-Menten constant; [S] is substrate concentration; [I] is inhibitor concentration, and K_i is the inhibition constant. Data were fitted using simultaneous nonlinear regression using Mathematica (Wolfram Research).

Glutaraldehyde Cross-linking—Bovine LPL and ANGPTL4 purified as above were buffer-exchanged into 20 mM HEPES, pH 8.0, 150 mM NaCl, 10% glycerol, 1 mM deoxycholate, and 1% Tween 20. 250 nM LPL was incubated between 0 and 5 μM ANGPTL4, or 100 nM ANGPTL4 was incubated with between 0 and 500 nM LPL for 10 min at room temperature. Glutaraldehyde was added to a final concentration of 0.25%, and the reaction was incubated at room temperature for 10 min. Cross-linking reactions were stopped with Tris, pH 8.0, to a final concentration of 150 mM and analyzed by Western blot as above.

Atomic Force Microscopy—100 nM LPL, 100 nM ANGPTL4, or 100 nM LPL plus 100 nM ANGPTL4 were incubated on ice for 15 min in 10 mM BisTris, pH 6.5, 500 nM NaCl, and 10% glycerol. Mixtures were diluted 5× into the same buffer, and 10 μl was immediately deposited onto freshly cleaved mica. The mica surface was then immediately washed with water, and a stream of nitrogen gas was used to dry the surface. Images were acquired with a Nanoscope III 3A atomic force microscope (Veeco, Santa Barbara, CA) in tapping mode with a resolution of 512 × 512 pixels at a scan rate of 1.97 Hz and over a 1 × 1 μm scan size. AFM tips were from NanoSensors (Neuchatel, Switzerland) with a spring constant between 21 and 98 N/m and resonance frequencies between 146 and 236 kHz. AFM images for each sample were consistent over multiple depositions (greater than three from each sample) and multiple tips (at least two for each deposition). Poor images resulting from blunted tips were excluded from analysis. Between three and five representative images of each sample condition were 3rd order plane-fitted and flattened using NanoScope Analysis version 1.40r1 (Bruker Instruments). Volume analysis of protein peaks was conducted with Image SXM 194-2X (Steve Barrett, University of Liverpool, UK) as described (30). Protein molecular mass was converted into predicted AFM volume using the following equation: $V = 1.2\cdot M - 14.7$, where V is AFM volume in nm^3, and M is molecular mass in kDa (31).

RESULTS

ANGPTL4 Is Not a Catalytic Inhibitor of LPL—The previously published model of LPL inhibition states that sub-stoichiometric quantities of ANGPTL4 to LPL are sufficient to completely inhibit LPL, and therefore, ANGPTL4 is a catalytic inhibitor of LPL (22). Our experiments, however, are not consistent with these results and reveal that super-stoichiometric ratios of ANGPTL4/LPL were needed for complete LPL inhibition. As is standard for LPL inhibition studies, the N-terminal coiled-coil domain of ANGPTL4 was used throughout this study, and we refer to it simply as ANGPTL4. In these experiments, a set amount of LPL was incubated on ice with varying amounts of ANGPTL4. Aliquots were removed at several time points over a 6-h period, and the lipase activity of LPL was measured (Fig. 1*A*). LPL without ANGPTL4 was also incubated on ice and used as the uninhibited control. Fig. 1*A* shows the fraction of control activity at the specified time points. Uninhibited LPL lost a total of 35% of its starting activity over the 6-h period. ANGPTL4 inhibited LPL in a dose-dependent manner within the first 15 min of the experiment. If ANGPTL4 is a catalytic inhibitor of LPL, we would expect an exponential

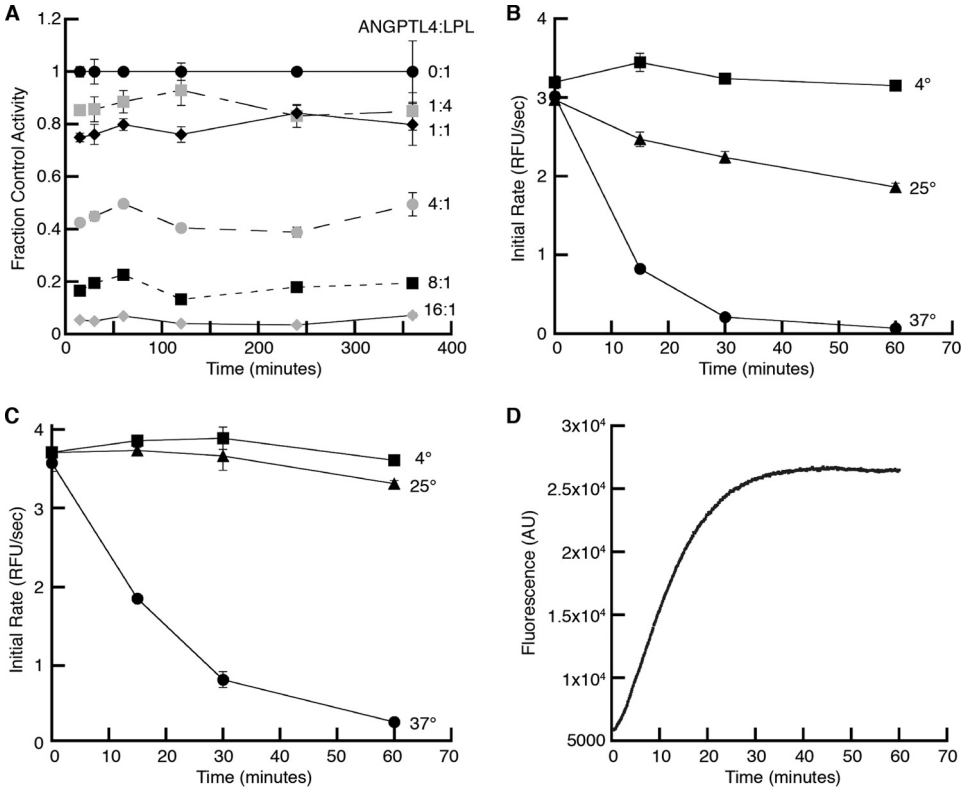

FIGURE 1. **Time course of LPL inhibition by ANGPTL4 and LPL inactivation by heat.** *A,* LPL (100 nM) was incubated on ice with ratios of ANGPTL4/LPL ranging from 0 to 16 ANGPTL4 monomers to 1 LPL dimer in buffer containing deoxycholate. Aliquots of the inhibition reactions were diluted 20 times into assay buffer, and the fraction of remaining LPL activity was assayed at several time points up to 6 h. For each time point, the inhibited reactions were normalized to the reaction without ANGPTL4. *B,* initial LPL activity was measured after incubation for various times at 4, 25, or 37 °C. *C,* deoxycholate stabilizes LPL as in *B*, except that 1 mM deoxycholate was added to the buffer. *D,* hydrophobic portions of LPL are exposed over time at 37 °C as shown by a fluorescence increase in a thermofluor assay. *RFU,* relative fluorescence units; *AU*, arbitrary units.

decay of LPL activity over time at sub-stoichiometric ratios of ANGPTL4 to LPL. However, we observed no additional LPL inhibition by ANGPTL4 after the first time point. Furthermore, an excess of ANGPTL4 monomers to LPL dimers was needed to see significant inhibition of lipase activity. These results indicate that ANGPTL4 is not a catalytic inhibitor of LPL.

Heat-inactivated LPL and ANGPTL4-inactivated LPL Are Not Equivalent—Temperature plays a key role in the stability of LPL *in vitro*. Even in the absence of ANGPTL4, LPL is rapidly inactivated at 37 °C unless accompanied by stabilizing factors such as deoxycholate (32). Fig. 1*B* shows a time course of LPL inactivation at several temperatures. As expected, deoxycholate (1 mM) stabilizes LPL against thermal inactivation as shown in Fig. 1*C*. LPL can be further protected at 37 °C by adding up to 5 mM deoxycholate to the LPL buffer (32). We also show the effects of heat on LPL inactivation with a fluorescence-based thermal stability assay (Thermofluor assay) (29, 33). In this assay, a hydrophobic fluoroprobe is quenched in solution, but fluorescence emission increases as the probe preferentially binds to the hydrophobic interior of an unfolded protein. We incubated LPL with the fluoroprobe at 37 °C for 2 h. Fluorescence steadily increased over time and reached a maximum after ~30 min (Fig. 1*D*), which corresponds to the nearly complete loss of lipase activity after 30 min seen in Fig. 1*B*. Taken together, these results indicate that although ANGPTL4 does not catalytically inactivate LPL, exposure to elevated temperatures results in rapid loss of LPL activity.

Active LPL dimers can be differentiated from inactive LPL monomers by their different binding affinities to heparin-Sepharose resin (34). Previously, it was suggested that heat-inactivated LPL binds heparin with the same affinity as ANGPTL4-inactivated LPL (22). It was also reported that ANGPTL4 binds heparin but with a lower affinity than either inactivated LPL or active LPL dimers (22). In an attempt to understand the mechanism of ANGPTL4 inactivation of LPL, we sought to purify ANGPTL4-inactivated LPL by heparin-Sepharose chromatography. However, in our experiments, we saw that heat-inactivated LPL bound with a distinctly lower affinity than ANGPTL4-inactivated LPL (Fig. 2).

Active LPL, heat-inactivated LPL, ANGPTL4-inactivated LPL, and ANGPTL4 were found to have distinct elution profiles on heparin-Sepharose chromatography. LPL samples were incubated on ice for 20 min, partially heat-inactivated at 37 °C for 20 min, or incubated with excess ANGPTL4 for 20 min. Samples were then assayed for lipase activity and separated using a salt gradient on a heparin-Sepharose column. The contents of the resulting fractions were analyzed by Western blot and lipase activity assays. First, the positions of active LPL and partially heat-inactivated LPL were established. Active LPL dimers eluted from the heparin column at ~1.36 M NaCl (Fig. 2*A*). Partially heat-inactivated LPL eluted from the column in two distinct peaks as follows: a peak of inactive LPL monomers at ~0.85 M NaCl and a peak of active LPL dimers at 1.36 M NaCl (Fig. 2*B*). Next, we analyzed LPL that had been partially inacti-

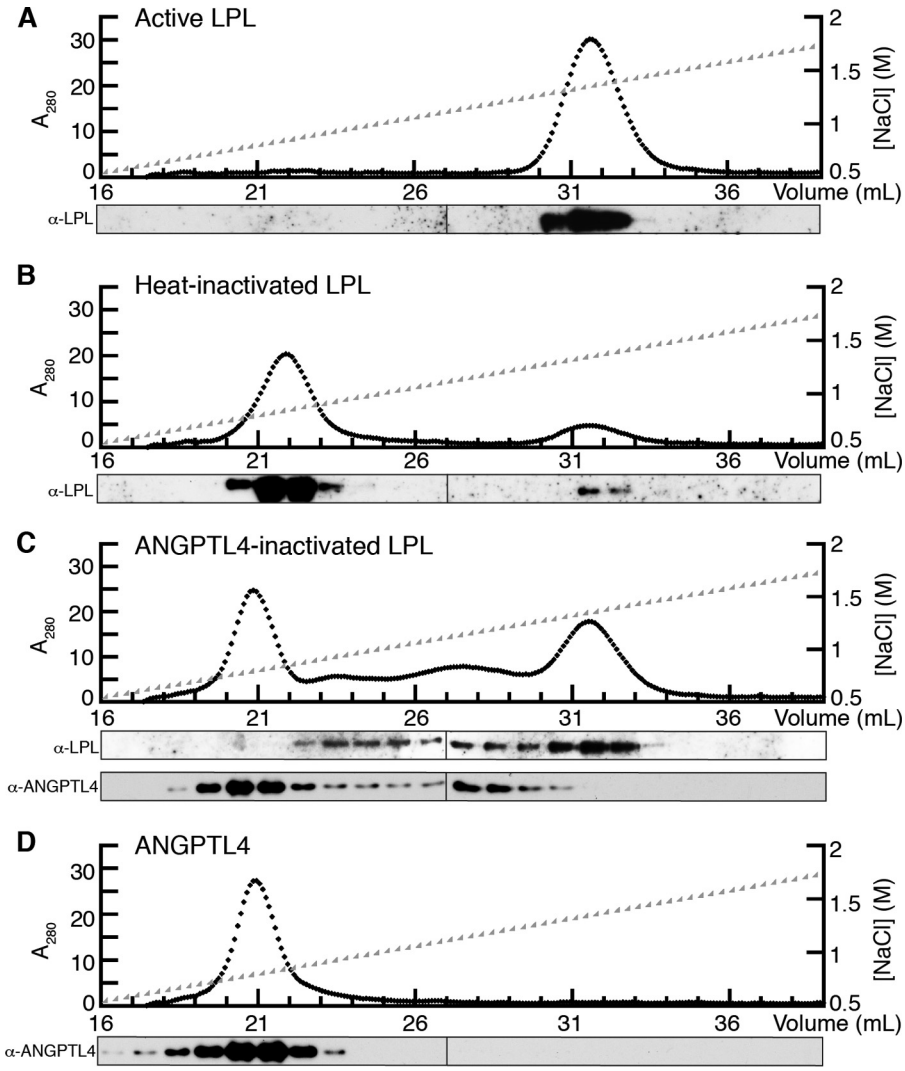

FIGURE 2. **Separation of active LPL, inactive LPL, and ANGPTL4 using heparin-Sepharose chromatography.** Equal amounts of active LPL (0.5 nmol), heat-inactivated LPL (0.5 nmol for 20 min at 37 °C), ANGPTL4-inactivated LPL (0.5 nmol of LPL with 12 nmol of ANGPTL4), or ANGPTL4 alone (12 nmol) were separated using a salt gradient using heparin-Sepharose chromatography. Western blots (shown *below each trace*) against LPL and/or ANGPTL4 were used to detect the specific protein present in each fraction. *A,* active LPL elutes late in the salt gradient. *B,* partial heat-inactivated LPL (20 min at 37 °C) elutes in two peaks. *C,* ANGPTL4 inactivation of LPL yields additional peaks that contain both LPL and ANGPTL4. *D,* ANGPTL4 alone elutes slightly before the heat-inactivated LPL peak.

vated by ANGPTL4 (Fig. 2*C*). Three distinct populations of proteins eluted from the column. First, a peak containing only ANGPTL4 eluted from the column at 0.78 M NaCl. Next, a set of peaks containing both LPL and ANGPTL4 eluted around 1.15 M NaCl, possibly showing multiple LPL-ANGPTL4 complexes. Finally, a peak containing only active LPL eluted at 1.36 M NaCl. ANGPTL4 alone was run as a reference (Fig. 2*D*), confirming that ANGPTL4 binds to heparin and elutes at ~0.78 M NaCl. These results show that ANGPTL4-inactivated LPL has a higher affinity for heparin-Sepharose than that of heat-inactivated LPL. In addition, ANGPTL4 remains bound to LPL in one or more catalytically inactive complexes that co-elute from a heparin-Sepharose column.

ANGPTL4-inactivated LPL Regains Activity after Heparin Chromatography—Protein mixtures were assayed for lipase activity before application to the heparin column, and eluate fractions were assayed after exiting the column. Fractions with elution volumes between 28 and 36 ml were the only fractions showing lipase activity (Fig. 3*A*). These fractions correspond to the active LPL peak eluting at 1.36 M NaCl. To directly compare the activity of LPL eluting off the column, we took the sum of the lipase activity of each fraction between 28 and 36 ml and normalized the total activity to the reference run with LPL incubated on ice. As shown in Fig. 3*B*, the partially heat-inactivated LPL entered the heparin column with ~30% of the lipase activity as that of the reference LPL. In Fig. 3*C*, the total LPL activity exiting the column from the partially heat-inactivated LPL remained constant at ~30% of the reference LPL activity. LPL that had been partially inactivated with ANGPTL4 showed ~15% of the reference lipase activity before entering the column. However, the total lipase activity exiting the column reached ~70% of the reference LPL activity. This result indicates that a portion of the LPL had dissociated from ANGPTL4 and recovered activity upon purification on a heparin column.

ANGPTL4 Inhibition of LPL Is Reversible—The recovery of LPL activity after heparin chromatography indicates that

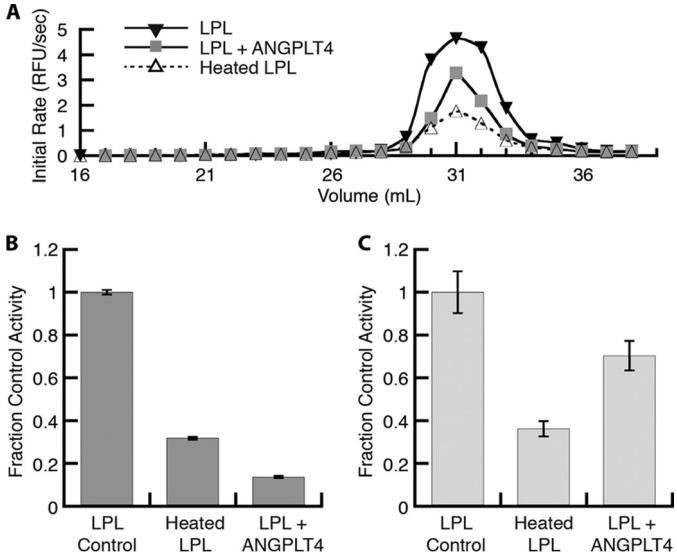

FIGURE 3. **LPL activity before and after heparin chromatography.** *A,* comparison of lipase activity by fraction in the untreated, heat-inactivated, and ANGPTL4-inactivated LPL samples. *B* and *C,* lipase activity of the heat-inactivated and ANGPTL4-inactivated LPL samples relative to the untreated LPL sample before (*B*) and after (*C*) separation by heparin chromatography. All active fractions for each sample in *A* were summed to generate relative activity in *C*. *RFU,* relative fluorescence units.

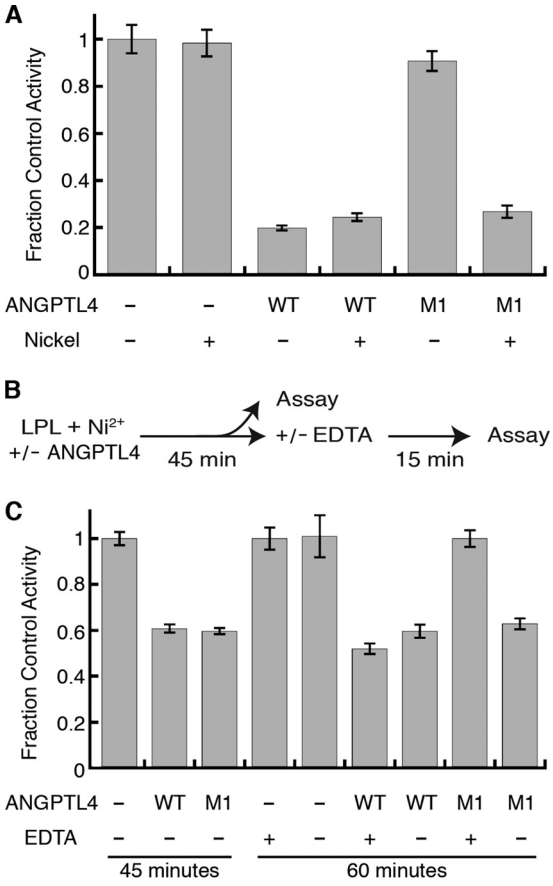

FIGURE 4. **MID1-ANGPTL4 requires nickel to be an effective inhibitor.** *A,* LPL incubated with WT-ANGPTL4 (*WT*) or MID1-ANGPTL4 (*M1*) with or without nickel ions. Initial rate of substrate hydrolysis for each sample was normalized to the sample containing LPL without ANGPTL4 or nickel. *B,* experimental scheme. LPL was inhibited for 45 min at 37 °C using WT or MID1-ANGPTL4 in the presence of 5 mM deoxycholate and Ni^{2+}. Samples were assayed for lipase activity and normalized to the positive control without ANGPTL4. Samples were then split; one fraction received EDTA, and one received an equal volume of water. Fractions were incubated for 15 min at 37 °C and were then assayed for lipase activity and normalized to the positive control (no ANGPTL4 and with EDTA). *C,* fraction remaining activity by sample where M1 is MID1-ANGPTL4.

ANGPTL4 inhibition of LPL is a reversible process rather than an irreversible unfolding reaction (22). This outcome was confirmed when we serendipitously generated a regulatable version of ANGPTL4 that is active in the presence of nickel ions and inactive in their absence. Metal-interface-design 1 (MID1) is a 5-kDa helical protein that forms homodimers mediated by metal ions (28). Working with N-terminally MID1-tagged ANGPTL4 (MID1-ANGPTL4), we noticed that, in the absence of a metal ion, MID1-ANGPTL4 had a reduced ability to inhibit LPL (Fig. 4*A*). Upon addition of nickel sulfate, MID1-ANGPTL4 was an equivalent inhibitor of LPL as compared with WT ANGPTL4. We also observed that addition of a chelator (EDTA) to nickel-containing MID1-ANGPTL4 hindered LPL inhibition back to the level of the apo-form.

We set out to exploit this property of MID1-ANGPTL4 to determine whether, through the addition and removal of nickel ions, we could inactivate or reactivate LPL at will. LPL inhibition reactions were set up according to the schematic in Fig. 4*B*. First, WT-ANGPTL4 or MID1-ANGPTL4, pre-mixed with nickel sulfate, was combined with LPL. LPL alone with nickel-containing ANGPTL4 buffer served as a positive control. At 45 min, an aliquot of each LPL mixture was assayed for lipase activity. Each mixture was then split in half, one-half receiving an excess of EDTA over nickel, and one-half receiving an equal volume of water. After 15 min, each mixture was assayed again. Before the addition of EDTA, both WT- and MID1-ANGPTL4 inhibited LPL to ~40% of the control activity (Fig. 4*C*). Addition of EDTA to the reaction mixtures had no effect on the lipase activity of the positive control or on WT-ANGPTL4's ability to inhibit LPL. However, EDTA did interrupt MID1-ANGPTL4 inhibition as LPL activity was restored to nearly 100% of the positive control. Using the MID1-tagged ANGPTL4, we were able to show that LPL inhibition by ANGPTL4 is fully reversible. Unlike earlier inhibition reactions, these reactions were carried out at 37 °C in the presence of the LPL-stabilizing agent deoxycholate (32). With the addition of 5 mM deoxycholate to the inhibition reactions, we were able to preserve 75% of the control lipase activity over 60 min at 37 °C. The reactions were performed at 37 °C to demonstrate that LPL inhibition by ANGPTL4 is reversible even at increased temperature and is distinct from thermal inactivation.

Molecular Mechanism of Inhibition—Once the reversibility of the ANGPTL4 inhibition reaction was established, we set out to better understand the mechanism of inhibition. Analysis of Michaelis-Menten curves at different inhibitor concentrations revealed that the V_{max} decreased with increasing inhibitor concentrations. The K_m for each inhibitor concentration varied slightly (with values of 1.4 ± 0.3 μM (no inhibitor) and 0.5 ± 0.1 μM (0.6 μM inhibitor), 0.7 ± 0.1 μM (1.8 μM inhibitor), 1.3 ± 0.2 μM (5.4 μM inhibitor), and 2.0 ± 0.3 μM (16.2 μM inhibitor), but it did not show a decreasing or increasing trend (Fig. 5). These results are most consistent with a noncompetitive mechanism of inhibition (35). Data from each inhibitor concentration were simultaneously fit to an equation for noncompetitive inhibition

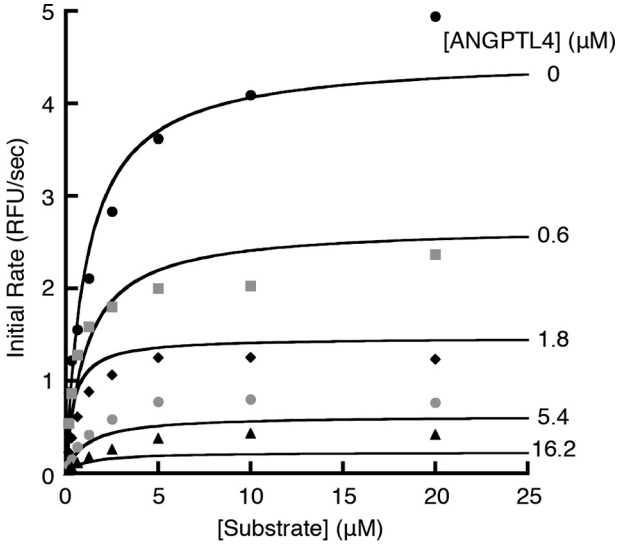

FIGURE 5. **ANGPTL4 inhibition of LPL is noncompetitive.** 12 nM LPL was incubated with between 0 and 16.3 μM ANGPTL4 for 10 min at room temperature in the presence of 1 mM deoxycholate. Inhibition reactions were diluted 2.4× into assay buffer, and the initial rate of substrate hydrolysis by LPL was recorded with increasing amounts of fluorescent substrate. *Solid lines* represent the best fit to an equation for noncompetitive inhibition solved simultaneously for all ANGPTL4 concentrations. *RFU,* relative fluorescence units.

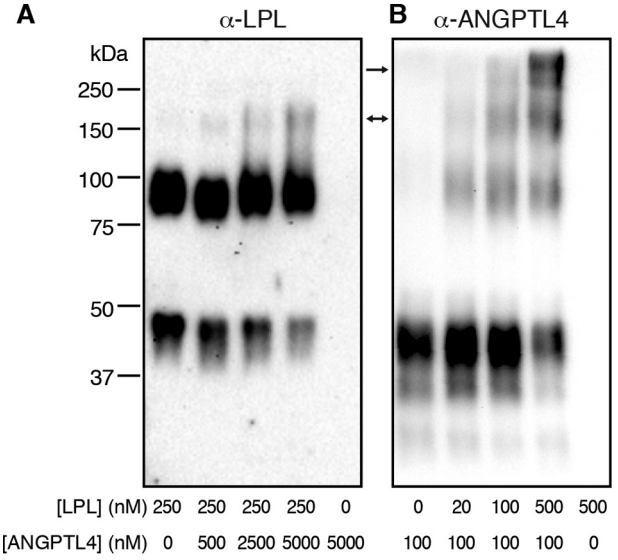

FIGURE 6. **Cross-linking reveals complexes of LPL and ANGPTL4.** *A,* LPL was incubated with increasing amounts of ANGPTL4, cross-linked using gluteraldehyde, and detected by Western blot using antibody against LPL. *B,* ANGPTL4 was incubated with increasing amounts of LPL, cross-linked using gluteraldehyde, and detected by Western blot using an ANGPTL4 antibody. *Arrows* point to the LPL-ANGPTL4 cross-linked complex.

($v = V_{max}\cdot[S]/\{(K_m\cdot(1 + [I]/K_i)) + ([S]\cdot(1+[I]/K_i))\}$ (31)) using nonlinear regression to yield a K_i of 0.86 ± 0.074 μM. To generate a more complete picture of ANGPTL4-inhibited LPL, we set out to measure the composition of the inhibited complex.

Composition of the Inhibited Complex—Our data show that complete inhibition of LPL by ANGPTL4 required multiple ANGPTL4 monomers per LPL dimer (Fig. 1*A*), that LPL and ANGPTL4 co-eluted during column chromatography (Fig. 2), and that inhibition is reversible (Figs. 3 and 4). These data are in contrast to the previous model in which ANGPTL4 acts as an unfolding molecular chaperone to yield inactive LPL monomers from active dimers. These contrasting models predict different molecular forms of inhibited LPL. Whereas ANGPTL4 acting catalytically as an unfolding molecular chaperone would increase LPL monomers and decrease LPL dimers, ANGPTL4 acting as a noncompetitive inhibitor would be expected to produce some higher molecular weight combination of LPL and ANGPTL4. We utilized AFM and protein-protein cross-linking to probe the stoichiometry of the inhibited complex.

For cross-linking experiments, LPL was first incubated with increasing amounts of ANGPTL4, cross-linked with glutaraldehyde, resolved by SDS-PAGE and detected by Western blot against LPL. LPL alone migrated mainly as dimers and monomers (migrating at ~50 and 100 kDa, Fig. 6*A*). When ANGPTL4 was added, a band of a higher molecular weight appeared. The molecular weight of this slowly migrating band appeared to be ~220 kDa, consistent with a complex of two ANGPTL4 tetramers (~60 kDa each) to one LPL dimer. The LPL antibody did not cross-react with the highest concentration of ANGPTL4 alone. Next, ANGPTL4 was incubated with increasing concentrations of LPL, and the position of ANGPTL4 was detected by Western blot (Fig. 6*B*). The apparent molecular weight of the ANGPTL4-reacting bands also shifted up such that two higher molecular weight bands were seen. In these experiments the antibody against ANGPTL4 did not detect the LPL alone.

We next utilized AFM to determine the distribution of oligomeric states of the inhibited LPL-ANGPTL4 complex in the absence of cross-linking. Volume analysis of AFM images has been shown to be a powerful tool for determining the oligomerization states of proteins, because the AFM volume depends linearly on the molecular weight of the protein (30, 31). ANGPTL4, LPL, and LPL-ANGPTL4 were imaged. Table 1 shows the predicted AFM volumes for various LPL and ANGPTL4 protein complexes. Images of ANGPTL4 alone yielded protein volumes ranging from 5 to 60 nm^3, which is consistent with ANGPTL4 dimers and tetramers (Fig. 7*A*). ANGPTL4 monomers may also be present, but with a predicted AFM volume of 3 nm^3, proteins of this size fall below the linear range of the AFM volume dependence on molecular weight. LPL alone showed a broad distribution of volumes between 60 and 110 nm^3, likely representing the dimer form (Fig. 7*B*). Topographical analysis of the LPL images show tightly spaced protein peaks, also indicative of dimeric proteins. A minor population of smaller particles was also seen, and we attribute these to an LPL cleavage fragment known to co-purify with full-length LPL. Addition of ANGPTL4 to LPL increased the observed volume of the protein particles (Fig. 7*C*). If ANGPTL4 catalytically transformed LPL dimers into LPL monomers, we would expect an increase in particles near the expected monomer volume of 46 nm^3. Furthermore, we would expect the distribution of ANGPTL4 protein volumes to remain between 5 and 60 nm^3. If ANGPTL4 and LPL did not interact at all, we would predict a combined volume distribution representing the ANGPTL4 distribution added to the LPL distribution. Instead, we see the volume of the main peak increase to between 110 and 160 nm^3. These AFM volumes could represent LPL dimers in complex with either ANGPTL4 monomers or ANGPTL4 dimers. They

TABLE 1

Predicted AFM volumes based on the linear dependency of AFM volume to protein molecular weight: $V = 1.2 \cdot M - 14.7$, where V is AFM volume in nm^3, and M is molecular mass in kDa

Protein complex	Mass	Predicted AFM volume (nm3)
	kDa	
ANGPTL4 monomer	15	3[a]
ANGPTL4 dimer[b]	31	22
ANGPTL4 tetramer[b]	62	59
LPL monomer	51	46
LPL dimer[c]	101	107
LPL monomer + ANGPTL4 monomer	66	65
LPL monomer + ANGPTL4 dimer	81	83
LPL monomer + ANGPTL4 tetramer[d]	112	120
LPL dimer + ANGPTL4 monomer[d]	117	125
LPL dimer + ANGPTL4 dimer[d]	132	144
LPL dimer + ANGPTL4 tetramer	163	181

[a] Out of linear range.
[b] ANGPTL4 dimers and tetramers are most likely represented in Fig. 7*A*.
[c] LPL dimers are seen in Fig. 7*B*.
[d] Possible LPL-ANGPTL4 complexes are seen in Fig. 7*C*.

could also correspond to LPL monomers in complex with ANGPTL4 tetramers. We believe this last option to be unlikely as there was a complete loss of the LPL dimer peak seen between 60 and 110 nm^3. With a 1:1 molar ratio of ANGPTL4 monomers to LPL dimers, there would not be sufficient ANGPTL4 tetramers to complex with each LPL monomer. By both cross-linking and AFM, we observed an increase in the molecular weight of LPL upon addition of ANGPTL4. This clearly indicates that ANGPTL4 does not simply monomerize LPL dimers but instead forms an LPL-ANGPTL4 complex.

DISCUSSION

Here, we demonstrate that ANGPTL4 is a reversible, noncompetitive inhibitor of LPL. Reversibility is demonstrated in two ways. First, the ANGPTL4-LPL complex partially dissociates during affinity chromatography, and active LPL is recovered. Second, we generated MID1-ANGPTL4, a regulatable variant of ANGPTL4. Use of MID1-ANGPTL4 showed that the metal-bound, functional form of MID1-ANGPTL4 inhibited LPL, but full LPL activity was recovered when MID1-ANGPTL4 was disabled by the addition of a chelator. After reversibility was demonstrated, inhibition kinetics were measured and found to be consistent with a noncompetitive mechanism. Finally, we show by AFM, protein-protein cross-linking, and column chromatography that the inhibited form of LPL is bound to ANGPTL4. Significantly, these data are consistent with a previous *in vivo* study showing that, in plasma from mice overexpressing ANGPTL4, ANGPTL4 and LPL form a complex as they co-migrate during heparin-Sepharose chromatography (36). Thus, our data show that ANGPTL4 acts as a conventional, noncompetitive inhibitor that binds to LPL and prevents it from hydrolyzing substrates.

Our data are in contrast to the previously published model for LPL inhibition by ANGPTL4 (Fig. 8) (22). By the earlier model, ANGPTL4 catalyzes a conformational switch of the active, dimeric LPL to an inactive, monomeric LPL. It was thus

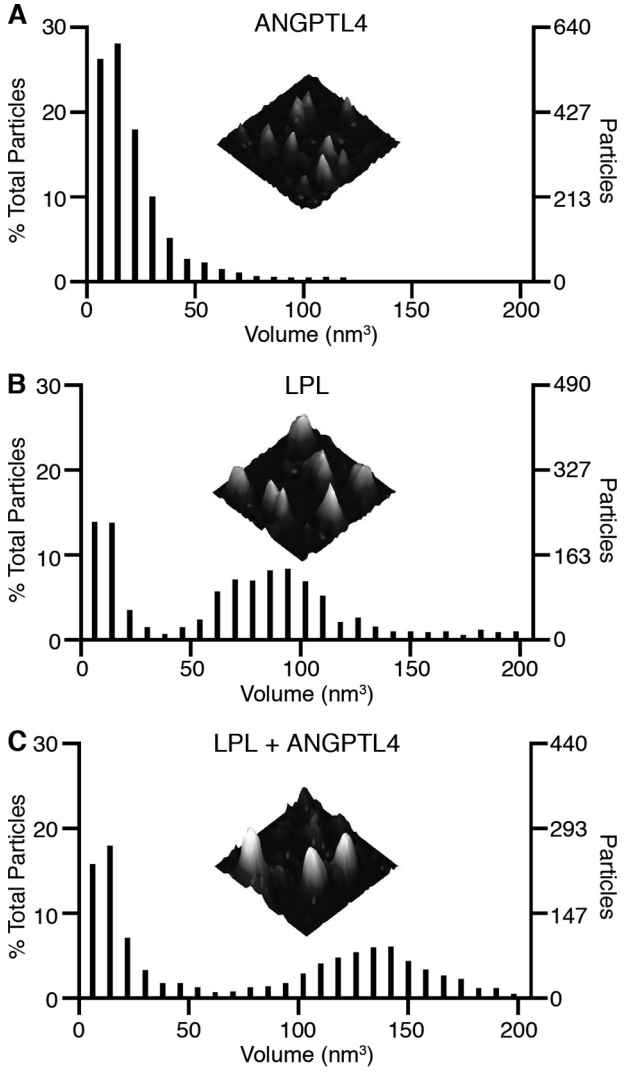

FIGURE 7. **Distribution of AFM particle volumes in cubic nanometers.** Particle distributions normalized by the percent of total particles in each size range. Topographical images correspond to an 80 × 80-nm area on the surface and between 0 and 1.5 nm off the surface. *A*, ANGPTL4 at 20 nM deposited onto a freshly cleaved mica surface and imaged with tapping mode AFM in air. Particles from four representative images from the same deposition and using the same tip were analyzed totaling 2150 particles. *B*, same as *A*., but with 20 nM LPL. Data from five representative images using the same tip totaling 1726 particles. *C*, LPL at 100 nM was combined with 100 nM ANGPTL4, incubated on ice for 15 min, then diluted to a final concentration of 20 nM LPL and 20 nM ANGPTL4. Samples were immediately deposited onto freshly cleaved mica and imaged as in *A* and *B*. Data from three representative images using the same tip total 1719 particles.

described as an unfolding molecular chaperone. However, unlike many unfolding molecular chaperones (37), ANGPTL4 does not utilize any external energy source such as ATP. The thermodynamics of this earlier model would require that active LPL exists in a higher energy form than inactive LPL and that ANGPTL4, through transient contact, could release this energy. We did see a rapid, irreversible loss of LPL activity when we incubated our inhibition reactions at 37 °C without stabilizing factors and hypothesize that thermal inactivation could account for these earlier results. It is well established that, in the absence of the stabilizing influence of its *in vivo* interacting partners, LPL requires additives such as deoxycholate and high salt to maintain activity during *in vitro* studies (26, 32, 38). For

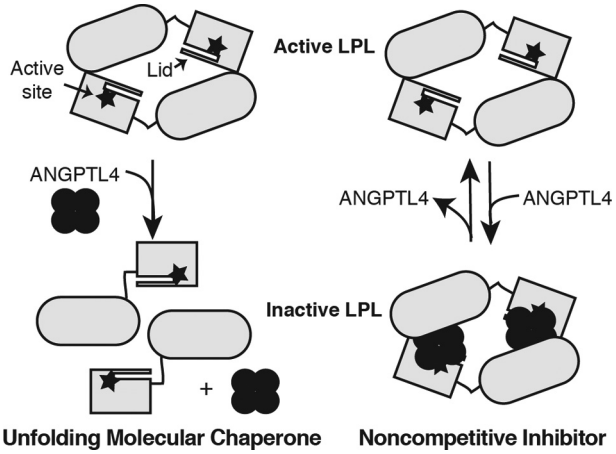

FIGURE 8. **Models for inhibition of LPL by ANGPTL4.** In the previous model, ANGPTL4 is thought to be an unfolding molecular chaperone, where ANGPTL4 irreversibly inactivates LPL, dissociates from LPL, and is free to inactivate additional LPL dimers. In the model presented here, ANGPTL4 is a noncompetitive inhibitor of LPL. ANGPTL4 bound to LPL is inactive, but activity is restored when ANGPTL4 is released from the LPL-ANGPTL4 complex.

this reason, all inhibition reactions done here are either incubated on ice or at 37 °C with deoxycholate to slow the spontaneous *in vitro* LPL inactivation. Furthermore, all inhibition experiments were corrected for this spontaneous LPL inactivation by using LPL alone as a control.

Mechanism of Inhibition—Analysis of ANGPTL4 inhibition kinetics reveals a noncompetitive mechanism. Noncompetitive inhibition effectively removes a portion of the enzyme from the reaction. This can occur by allosteric distortion of the active site upon inhibitor binding, which does not prevent substrate binding but renders the enzyme catalytically inactive (35). Alternatively, noncompetitive inhibitors can bind at sites other than the active site but sterically block substrate access (35, 39). Both models represent possible noncompetitive mechanisms for inhibition because they do not compete with substrate for the active site of the enzyme. Sites in LPL for allosteric inhibition by ANGPTL4 are currently not known. A possible model for inhibition by steric block is that ANGPTL4 could bind to the LPL lid region and prevent LPL from accessing substrate. Distinguishing the precise mechanisms of ANGPTL4 inhibition of LPL will require further analysis of the LPL-ANGPTL4 interaction.

Physiological Consequences of Reversible ANGPTL4 Inhibition—The precise cellular location where LPL inhibition occurs is currently unresolved. Although LPL functions on the apical face of capillary endothelial cells, it is not made by the endothelial cells but rather the underlying adipocyte or myocyte cells (40). The protein GPIHBP1 binds to the endothelium of capillary cells where it provides a platform for LPL to process triglycerides from lipoproteins (41). GPIHBP1 also helps transport LPL across the endothelial cells, and a recent study has shown that this transport is bidirectional (25, 42). ANGPTL4 could thus inhibit LPL in either the subendothelial space or on the surface of the capillary endothelium, and a number of recent studies support the former option. First, although ANGPTL4 is known to regulate LPL activity *in vivo* and *in vitro*, two studies in human populations found no correlation between serum ANGPTL4 and triglyceride levels (24, 43). Full-length ANGPTL4 is known to interact with the extracellular matrix in the subendothelial space via its C-terminal domain (44). Next, serum lipoproteins have been shown to prevent inhibition of LPL by ANGPTL4, and it is estimated that the concentration of circulating lipoproteins would be sufficient to prevent inhibition on the apical face of the capillary cells (45). GPIHBP1 also protects LPL against inhibition by ANGPTL4, and GPIHBP1 is made by endothelial cells and found both on their apical and basolateral surfaces (38, 41).

These findings, combined with our model for reversible inhibition of LPL, evoke the possibility that ANGPTL4 could sequester LPL in the subendothelial space. By this model, ANGPTL4 binding to LPL could prevent its movement to the apical face of endothelial cells. Inhibition could be reversed and active LPL released when appropriate nutritional cues emerged. We can only speculate on the nature of these cues, but certain biological molecules such as free fatty acids reduce ANGPTL4 inhibition of LPL (46). Because fatty acids are mobilized to the circulation from adipose tissue upon fasting (47), they are unlikely to be the specific cue that releases ANGPTL4 inhibition of LPL. However, a small molecule capable of reversing ANGPTL4 inhibition of LPL provides an appealing model for nutritionally responsive LPL regulation.

Although further studies will be required to understand the significance of reversible LPL inhibition by ANGPTL4 *in vivo*, achieving this understanding is important because genetic studies in humans strongly support a role for ANGPTL4 in regulation of plasma triglyceride levels. A naturally occurring sequence variant of ANGPTL4, E40K, is present in 3% of European-Americans. This variant is found to be significantly associated with lower plasma triglycerides and higher HDL-C (43, 48), an athero-protective lipid profile. It is thus likely that ANGPTL4 is a prime pharmacological target for the treatment of hypertriglyceridemia (6). For example, inhibiting ANGPTL4 with a neutralizing antibody lowered plasma triglyceride levels in hypertriglyceridemic mice, and such antibodies are suggested to have potential therapeutic applications in dyslipidemia (49). For these studies, a more complete understanding of the activity and availability of the cellular pools of LPL is necessary.

Acknowledgments—We thank Charles Carter, Robert Sauer, and Richard Wolfenden for helpful discussions; Brian Kuhlman and Ciara Gallagher for suggestions on the manuscript; Bryan Der for the MID1 tag; Caterina Schweidenback and Shawn Hendersen for help with modeling in Mathematica, and Julia Medland for technical assistance with AFM.

REFERENCES

1. Mead, J. R., Irvine, S. A., and Ramji, D. P. (2002) Lipoprotein lipase: structure, function, regulation, and role in disease. *J. Mol. Med.* **80,** 753–769
2. Johansen, C. T., and Hegele, R. A. (2011) Genetic bases of hypertriglyceridemic phenotypes. *Curr. Opin. Lipidol.* **22,** 247–253
3. Nichols, G. A., Arondekar, B., and Garrison, L. P., Jr. (2011) Patient characteristics and medical care costs associated with hypertriglyceridemia. *Am. J. Cardiol.* **107,** 225–229
4. Miller, M., Stone, N. J., Ballantyne, C., Bittner, V., Criqui, M. H., Ginsberg, H. N., Goldberg, A. C., Howard, W. J., Jacobson, M. S., Kris-Etherton, P. M., Lennie, T. A., Levi, M., Mazzone, T., and Pennathur, S. (2011)

Triglycerides and cardiovascular disease: a scientific statement from the American Heart Association. *Circulation* **123,** 2292–2333
5. D'Agostino, R. B., Jr., Hamman, R. F., Karter, A. J., Mykkanen, L., Wagenknecht, L. E., and Haffner, S. M. (2004) Cardiovascular disease risk factors predict the development of type 2 diabetes: the insulin resistance atherosclerosis study. *Diabetes Care* **27,** 2234–2240
6. Kersten, S. (2005) Regulation of lipid metabolism via angiopoietin-like proteins. *Biochem. Soc. Trans.* **33,** 1059–1062
7. Gaudet, D., Méthot, J., Déry, S., Brisson, D., Essiembre, C., Tremblay, G., Tremblay, K., de Wal, J., Twisk, J., van den Bulk, N., Sier-Ferreira, V., and van Deventer, S. (2013) Efficacy and long-term safety of alipogene tiparvovec (AAV1-LPLS447X) gene therapy for lipoprotein lipase deficiency: an open-label trial. *Gene Ther.* **20,** 361–369
8. Wong, H., and Schotz, M. C. (2002) The lipase gene family. *J. Lipid Res.* **43,** 993–999
9. Kobayashi, Y., Nakajima, T., and Inoue, I. (2002) Molecular modeling of the dimeric structure of human lipoprotein lipase and functional studies of the carboxyl-terminal domain. *Eur. J. Biochem.* **269,** 4701–4710
10. Bourne, Y., Martinez, C., Kerfelec, B., Lombardo, D., Chapus, C., and Cambillau, C. (1994) Horse pancreatic lipase. The crystal structure refined at 2.3 Å resolution. *J. Mol. Biol.* **238,** 709–732
11. Gin, P., Goulbourne, C. N., Adeyo, O., Beigneux, A. P., Davies, B. S., Tat, S., Voss, C. V., Bensadoun, A., Fong, L. G., and Young, S. G. (2012) Chylomicronemia mutations yield new insights into interactions between lipoprotein lipase and GPIHBP1. *Hum. Mol. Genet.* **21,** 2961–2972
12. Lookene, A., Zhang, L., Hultin, M., and Olivecrona, G. (2004) Rapid subunit exchange in dimeric lipoprotein lipase and properties of the inactive monomer. *J. Biol. Chem.* **279,** 49964–49972
13. Wong, H., Yang, D., Hill, J. S., Davis, R. C., Nikazy, J., and Schotz, M. C. (1997) A molecular biology-based approach to resolve the subunit orientation of lipoprotein lipase. *Proc. Natl. Acad. Sci. U.S.A.* **94,** 5594–5598
14. Ruge, T., Svensson, M., Eriksson, J. W., and Olivecrona, G. (2005) Tissue-specific regulation of lipoprotein lipase in humans: effects of fasting. *Eur. J. Clin. Invest.* **35,** 194–200
15. Kersten, S., Mandard, S., Tan, N. S., Escher, P., Metzger, D., Chambon, P., Gonzalez, F. J., Desvergne, B., and Wahli, W. (2000) Characterization of the fasting-induced adipose factor FIAF, a novel peroxisome proliferator-activated receptor target gene. *J. Biol. Chem.* **275,** 28488–28493
16. Köster, A., Chao, Y. B., Mosior, M., Ford, A., Gonzalez-DeWhitt, P. A., Hale, J. E., Li, D., Qiu, Y., Fraser, C. C., Yang, D. D., Heuer, J. G., Jaskunas, S. R., and Eacho, P. (2005) Transgenic angiopoietin-like (angptl)4 overexpression and targeted disruption of angptl4 and angptl3: regulation of triglyceride metabolism. *Endocrinology* **146,** 4943–4950
17. Yoshida, K., Shimizugawa, T., Ono, M., and Furukawa, H. (2002) Angiopoietin-like protein 4 is a potent hyperlipidemia-inducing factor in mice and inhibitor of lipoprotein lipase. *J. Lipid Res.* **43,** 1770–1772
18. Ge, H., Yang, G., Huang, L., Motola, D. L., Pourbahrami, T., and Li, C. (2004) Oligomerization and regulated proteolytic processing of angiopoietin-like protein 4. *J. Biol. Chem.* **279,** 2038–2045
19. Lei, X., Shi, F., Basu, D., Huq, A., Routhier, S., Day, R., and Jin, W. (2011) Proteolytic processing of angiopoietin-like protein 4 by proprotein convertases modulates its inhibitory effects on lipoprotein lipase activity. *J. Biol. Chem.* **286,** 15747–15756
20. Ge, H., Yang, G., Yu, X., Pourbahrami, T., and Li, C. (2004) Oligomerization state-dependent hyperlipidemic effect of angiopoietin-like protein 4. *J. Lipid Res.* **45,** 2071–2079
21. Yin, W., Romeo, S., Chang, S., Grishin, N. V., Hobbs, H. H., and Cohen, J. C. (2009) Genetic variation in ANGPTL4 provides insights into protein processing and function. *J. Biol. Chem.* **284,** 13213–13222
22. Sukonina, V., Lookene, A., Olivecrona, T., and Olivecrona, G. (2006) Angiopoietin-like protein 4 converts lipoprotein lipase to inactive monomers and modulates lipase activity in adipose tissue. *Proc. Natl. Acad. Sci. U.S.A.* **103,** 17450–17455
23. Osborne, J. C., Jr., Bengtsson-Olivecrona, G., Lee, N. S., and Olivecrona, T. (1985) Studies on inactivation of lipoprotein lipase: role of the dimer to monomer dissociation. *Biochemistry* **24,** 5606–5611
24. Robciuc, M. R., Tahvanainen, E., Jauhiainen, M., and Ehnholm, C. (2010) Quantitation of serum angiopoietin-like proteins 3 and 4 in a Finnish population sample. *J. Lipid Res.* **51,** 824–831
25. Davies, B. S., Goulbourne, C. N., Barnes, R. H., 2nd, Turlo, K. A., Gin, P., Vaughan, S., Vaux, D. J., Bensadoun, A., Beigneux, A. P., Fong, L. G., and Young, S. G. (2012) Assessing mechanisms of GPIHBP1 and lipoprotein lipase movement across endothelial cells. *J. Lipid Res.* **53,** 2690–2697
26. Bengtsson-Olivecrona, G., and Olivecrona, T. (1991) Phospholipase activity of milk lipoprotein lipase. *Methods Enzymol.* **197,** 345–356
27. Shan, L., Yu, X. C., Liu, Z., Hu, Y., Sturgis, L. T., Miranda, M. L., and Liu, Q. (2009) The angiopoietin-like proteins ANGPTL3 and ANGPTL4 inhibit lipoprotein lipase activity through distinct mechanisms. *J. Biol. Chem.* **284,** 1419–1424
28. Der, B. S., Machius, M., Miley, M. J., Mills, J. L., Szyperski, T., and Kuhlman, B. (2012) Metal-mediated affinity and orientation specificity in a computationally designed protein homodimer. *J. Am. Chem. Soc.* **134,** 375–385
29. Ericsson, U. B., Hallberg, B. M., Detitta, G. T., Dekker, N., and Nordlund, P. (2006) Thermofluor-based high-throughput stability optimization of proteins for structural studies. *Anal. Biochem.* **357,** 289–298
30. Ratcliff, G. C., and Erie, D. A. (2001) A novel single-molecule study to determine protein–protein association constants. *J. Am. Chem. Soc.* **123,** 5632–5635
31. Yang, Y., Wang, H., and Erie, D. A. (2003) Quantitative characterization of biomolecular assemblies and interactions using atomic force microscopy. *Methods* **29,** 175–187
32. Bengtsson, G., and Olivecrona, T. (1979) Binding of deoxycholate to lipoprotein lipase. *Biochim. Biophys. Acta* **575,** 471–474
33. Pantoliano, M. W., Petrella, E. C., Kwasnoski, J. D., Lobanov, V. S., Myslik, J., Graf, E., Carver, T., Asel, E., Springer, B. A., Lane, P., and Salemme, F. R. (2001) High-density miniaturized thermal shift assays as a general strategy for drug discovery. *J. Biomol. Screen.* **6,** 429–440
34. Peterson, J., Fujimoto, W. Y., and Brunzell, J. D. (1992) Human lipoprotein lipase: relationship of activity, heparin affinity, and conformation as studied with monoclonal antibodies. *J. Lipid Res.* **33,** 1165–1170
35. Segel, I. H. (1975) *Enzyme Kinetics: Behavior and Analysis of Rapid Equilibrium and Steady State Enzyme Systems*, pp. 125–135, John Wiley & Sons, Inc., New York
36. Lichtenstein, L., Berbée, J. F., van Dijk, S. J., van Dijk, K. W., Bensadoun, A., Kema, I. P., Voshol, P. J., Müller, M., Rensen, P. C., and Kersten, S. (2007) Angptl4 upregulates cholesterol synthesis in liver via inhibition of LPL- and HL-dependent hepatic cholesterol uptake. *Arterioscler. Thromb. Vasc. Biol.* **27,** 2420–2427
37. Liberek, K., Lewandowska, A., and Zietkiewicz, S. (2008) Chaperones in control of protein disaggregation. *EMBO J.* **27,** 328–335
38. Sonnenburg, W. K., Yu, D., Lee, E. C., Xiong, W., Gololobov, G., Key, B., Gay, J., Wilganowski, N., Hu, Y., Zhao, S., Schneider, M., Ding, Z. M., Zambrowicz, B. P., Landes, G., Powell, D. R., and Desai, U. (2009) GPIHBP1 stabilizes lipoprotein lipase and prevents its inhibition by angiopoietin-like 3 and angiopoietin-like 4. *J. Lipid Res.* **50,** 2421–2429
39. Arias, H. R., Bhumireddy, P., and Bouzat, C. (2006) Molecular mechanisms and binding site locations for noncompetitive antagonists of nicotinic acetylcholine receptors. *Int. J. Biochem. Cell Biol.* **38,** 1254–1276
40. Wang, H., and Eckel, R. H. (2009) Lipoprotein lipase: from gene to obesity. *Am. J. Physiol. Endocrinol. Metab.* **297,** E271–E288
41. Beigneux, A. P., Davies, B. S., Gin, P., Weinstein, M. M., Farber, E., Qiao, X., Peale, F., Bunting, S., Walzem, R. L., Wong, J. S., Blaner, W. S., Ding, Z. M., Melford, K., Wongsiriroj, N., Shu, X., de Sauvage, F., Ryan, R. O., Fong, L. G., Bensadoun, A., and Young, S. G. (2007) Glycosylphosphatidylinositol-anchored high-density lipoprotein-binding protein 1 plays a critical role in the lipolytic processing of chylomicrons. *Cell Metab.* **5,** 279–291
42. Davies, B. S., Beigneux, A. P., Barnes, R. H., 2nd, Tu, Y., Gin, P., Weinstein, M. M., Nobumori, C., Nyrén, R., Goldberg, I., Olivecrona, G., Bensadoun, A., Young, S. G., and Fong, L. G. (2010) GPIHBP1 is responsible for the entry of lipoprotein lipase into capillaries. *Cell Metab.* **12,** 42–52
43. Smart-Halajko, M. C., Robciuc, M. R., Cooper, J. A., Jauhiainen, M., Kumari, M., Kivimaki, M., Khaw, K. T., Boekholdt, S. M., Wareham, N. J., Gaunt, T. R., Day, I. N., Braund, P. S., Nelson, C. P., Hall, A. S., Samani,

N. J., Humphries, S. E., Ehnholm, C., and Talmud, P. J. (2010) The relationship between plasma angiopoietin-like protein 4 levels, angiopoietin-like protein 4 genotype, and coronary heart disease risk. *Arterioscler. Thromb. Vasc. Biol.* **30,** 2277–2282

44. Cazes, A., Galaup, A., Chomel, C., Bignon, M., Bréchot, N., Le Jan, S., Weber, H., Corvol, P., Muller, L., Germain, S., and Monnot, C. (2006) Extracellular matrix-bound angiopoietin-like 4 inhibits endothelial cell adhesion, migration, and sprouting and alters actin cytoskeleton. *Circ. Res.* **99,** 1207–1215
45. Nilsson, S. K., Anderson, F., Ericsson, M., Larsson, M., Makoveichuk, E., Lookene, A., Heeren, J., and Olivecrona, G. (2012) Triacylglycerol-rich lipoproteins protect lipoprotein lipase from inactivation by ANGPTL3 and ANGPTL4. *Biochim. Biophys. Acta* **1821,** 1370–1378
46. Robal, T., Larsson, M., Martin, M., Olivecrona, G., and Lookene, A. (2012) Fatty acids bind tightly to the N-terminal domain of angiopoietin-like protein 4 and modulate its interaction with lipoprotein lipase. *J. Biol. Chem.* **287,** 29739–29752
47. Lafontan, M., and Langin, D. (2009) Lipolysis and lipid mobilization in human adipose tissue. *Prog. Lipid Res.* **48,** 275–297
48. Romeo, S., Pennacchio, L. A., Fu, Y., Boerwinkle, E., Tybjaerg-Hansen, A., Hobbs, H. H., and Cohen, J. C. (2007) Population-based resequencing of ANGPTL4 uncovers variations that reduce triglycerides and increase HDL. *Nat. Genet.* **39,** 513–516
49. Desai, U., Lee, E. C., Chung, K., Gao, C., Gay, J., Key, B., Hansen, G., Machajewski, D., Platt, K. A., Sands, A. T., Schneider, M., Van Sligtenhorst, I., Suwanichkul, A., Vogel, P., Wilganowski, N., Wingert, J., Zambrowicz, B. P., Landes, G., and Powell, D. R. (2007) Lipid-lowering effects of anti-angiopoietin-like 4 antibody recapitulate the lipid phenotype found in angiopoietin-like 4 knockout mice. *Proc. Natl. Acad. Sci. U.S.A.* **104,** 11766–11771